RhoGDI2 suppresses lung metastasis in mice by reducing tumor versican expression and macrophage infiltration

Neveen Said,[1] Marta Sanchez-Carbayo,[2] Steven C. Smith,[1] and Dan Theodorescu[3,4]

[1]Department of Urology, University of Virginia, Charlottesville, Virginia, USA. [2]Spanish National Cancer Institute (CNIO), Madrid, Spain.
[3]Department of Surgery and Department of Pharmacology, University of Colorado, Aurora, Colorado, USA.
[4]University of Colorado Comprehensive Cancer Center, Aurora, Colorado, USA.

Half of patients with muscle-invasive bladder cancer develop metastatic disease, and this is responsible for most of the deaths from this cancer. Low expression of RhoGTP dissociation inhibitor 2 (RhoGDI2; also known as ARHGDIB and Ly-GDI) is associated with metastatic disease in patients with muscle-invasive bladder cancer. Moreover, a reduction in metastasis is observed upon reexpression of RhoGDI2 in xenograft models of metastatic cancer. Here, we show that RhoGDI2 suppresses lung metastasis in mouse models by reducing the expression of isoforms V1 and V3 of the proteoglycan versican (VCAN; also known as chondroitin sulfate proteoglycan 2 [CSPG2]). In addition, we found that high versican levels portended poor prognosis in patients with bladder cancer. The functional importance of tumor expression of versican in promoting metastasis was established in in vitro and in vivo studies in mice that implicated a role for the chemokine CCL2 (also known as MCP1) and macrophages. Further analysis indicated that RhoGDI2 suppressed metastasis by altering inflammation in the tumor microenvironment. In summary, we demonstrate what we believe to be a new mechanism of metastasis suppression that works by reducing host responses that promote metastatic colonization of the lung. Therapeutic targeting of these interactions may provide a novel adjuvant strategy for delaying the appearance of clinical metastasis in patients.

Introduction

One-half of patients with muscle-invasive (MI) urothelial cancer (UC) of the bladder develop distant metastases, even after radical surgery of the primary tumors. We identified RhoGTP dissociation inhibitor 2 (RhoGDI2; also known as ARHGDIB and Ly-GDI, and abbreviated herein as GDI2) as an invasion and metastasis suppressor in human bladder cancer cell lines (1) and have shown that its expression is inversely associated with clinical outcome after treatment of MI tumors (2). Independently, in comparative gene expression profiling of invasive bladder cancer cell lines and human MI UC samples, we identified versican (VCAN; also known as chondroitin sulfate proteoglycan 2, [CSPG2]) as highly expressed in invasive and metastatic cancers (3).

Versican is a highly conserved structural component of the ECM that is involved in neuronal development (4–8), the inflammatory phase of pulmonary-vascular diseases, atherosclerosis (9–12), and the invasive and metastatic signatures of many cancers (13–25). Four isoforms or spliced variants have been reported for versican, and the roles of V0, V1, and V3 and to a lesser extent V2 isoforms are recognized in cancer, vascular disease, and neuronal development (detailed in refs. 8, 26, 27, and the references cited therein). These isoforms contribute to proliferative, adhesive, and migratory states of tumor cells and modulate their interactions with stroma in the tumor microenvironment (26, 28, 29).

Versican expression is regulated by cytokines, chemokines, and hypoxia (6, 7, 9–12, 21, 26, 29–36) via transcription factors such as TCF-4, SP-1, AP-1, and p53, which have binding motifs in the versican promoter (5, 19, 27, 36–38). Versican promoter upregulation via AP-1 accounts for the higher mRNA expression levels observed in invasive human melanoma cells (36, 39). TCF-4 has been reported to control the expression of versican isoforms in prostate cancer cells (19, 27, 38).

Here, we demonstrate what we believe is a novel mechanism of metastasis suppression by showing that the metastasis suppressor activity of GDI2 is dependent on a reduction of versican expression. Experiments with human and murine xenografts in the context of pharmacologic and genetic manipulation using transgenic mice suggested that both CCL2 and macrophages were necessary for versican to exert its metastasis-promoting role. We believe this work is the first demonstration of a tumor metastasis suppressor blocking the prometastatic inflammatory host response in a distant organ and, by virtue of this fact, highlights the therapeutic potential of targeting both malignant and host-derived components of the tumor microenvironment.

Results

Versican is a putative effector of the GDI2 metastasis suppressor. Reduced mRNA expression of GDI2 is associated with poor clinical outcome in UC (Figure 1A). Since recent reports found that regulation of transcription may be central in metastasis suppressor gene function (40, 41), we used a transcriptional screen to identify putative effectors of GDI2. We compared gene expression by high-density oligonucleotide microarrays of low GDI2–expressing and highly metastatic UMUC3 cells previously (42) transfected with a GFP-GDI2 (GFP) fusion protein to those harboring a GFP vector alone. Reexpression of GDI2 in these cells leads to a significant reduction in metastatic colonization of the lung (42).

Conflict of interest: The authors have declared that no conflict of interest exists.
Citation for this article: *J Clin Invest.* 2012;122(4):1503–1518. doi:10.1172/JCI61392.

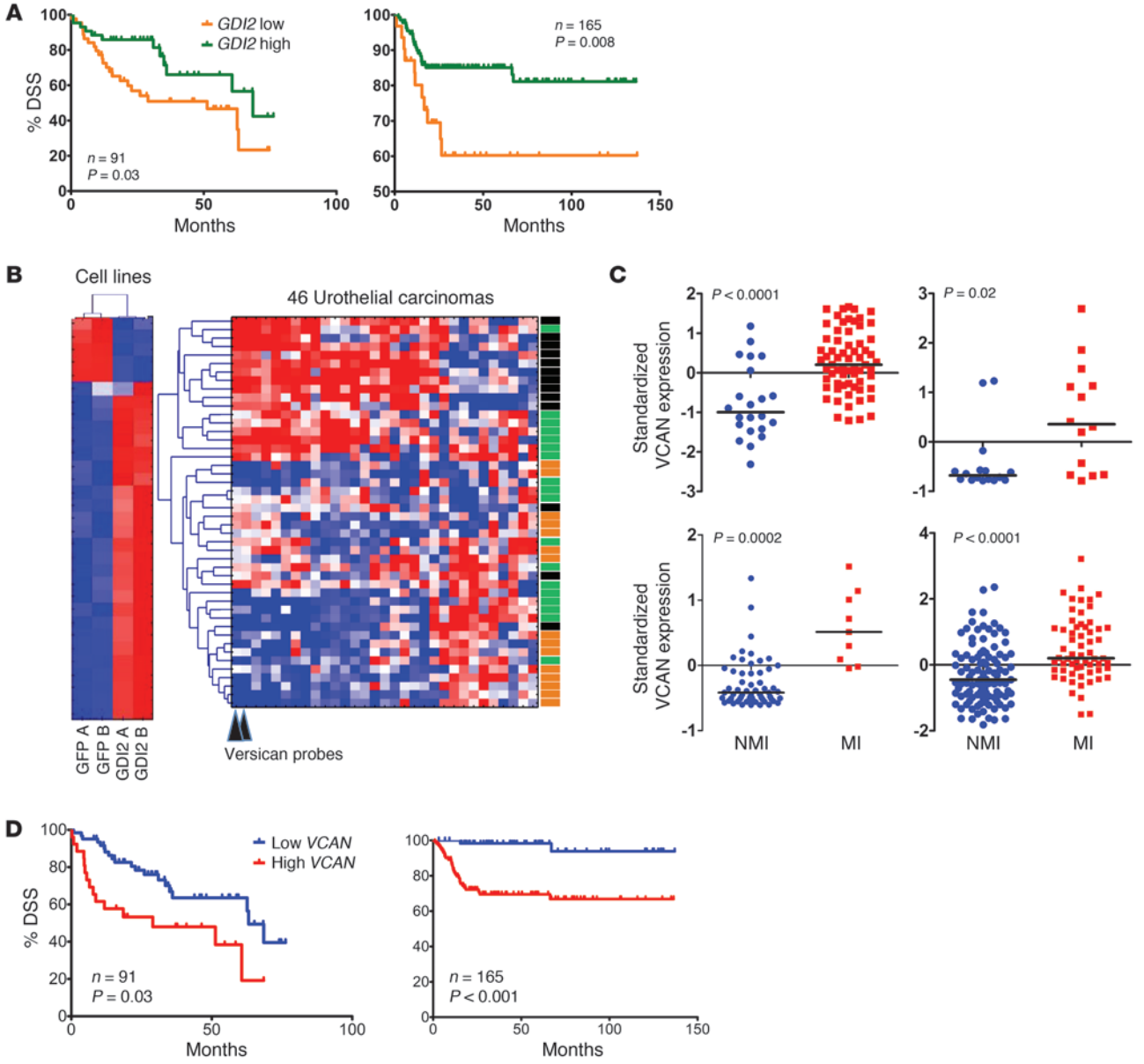

Figure 1

GDI2 and versican expression and disease outcome. (**A**) Kaplan-Meier curves showing stratification of DSS as a function of GDI2 RNA expression in 2 independent studies (left: Sanchez-Carbayo et al., ref. 44; right: Kim et al., ref. 46). (**B**) Supervised clustering of microarray analysis of metastatic UMUC3 cells reexpressing GDI2-GFP and GFP controls was limited to 92 significantly differentially expressed probes by more than 3-fold (right). Unsupervised clustering of 92 GDI2-regulated probes in 46 human urothelial carcinomas (43) (left). Stage of the tumor is classified as carcinoma in situ (green), NMI (orange), and MI (black) urothelial bladder cancer. Probes for *VCAN* mRNA are indicated by arrowheads. (**C**) Dot plots of standardized (*z* scored), logged (base 2) expression of VCAN probes comparing NMI and MI urothelial bladder cancer in 4 independent studies shown (upper left: Sanchez-Carbayo et al., ref. 44; upper right: Stransky et al., ref. 45; lower left: Dyrskjot et al., ref. 47; lower right: Kim et al., ref. 46). Differences in distributions were tested by the Mann-Whitney *U* test. (**D**) Kaplan-Meier plots showing stratification of DSS as a function of VCAN expression in the same 2 studies as in **A** (left: Sanchez-Carbayo et al., ref. 44; right: Kim et al., ref. 46). Reproduced with permission from the *Journal of Clinical Oncology* (44), *Molecular Cancer* (46), *Cancer Research* (43), and *Nature Genetics* (45, 47).

This comparison identified 92 significantly differentially expressed probes by a more than 3-fold change. Given the role of GDI2 in suppression of invasion and metastasis (1), we restricted further analysis to candidates significantly associated with MI disease in a cohort of UCs ($n = 46$) profiled by microarray (ref. 43 and Figure 1B). Using hierarchical clustering analysis to examine the pattern of expression of these probes in the human tumors, we observed the pattern of GDI2-regulated genes related to disease stage (Figure 1B). Interestingly, versican was the most repressed by reexpression of GDI2 (fold change > 8-fold) while being the most significantly overexpressed in invasive as compared with noninvasive cancer. Supporting the notion that GDI2 represses versi-

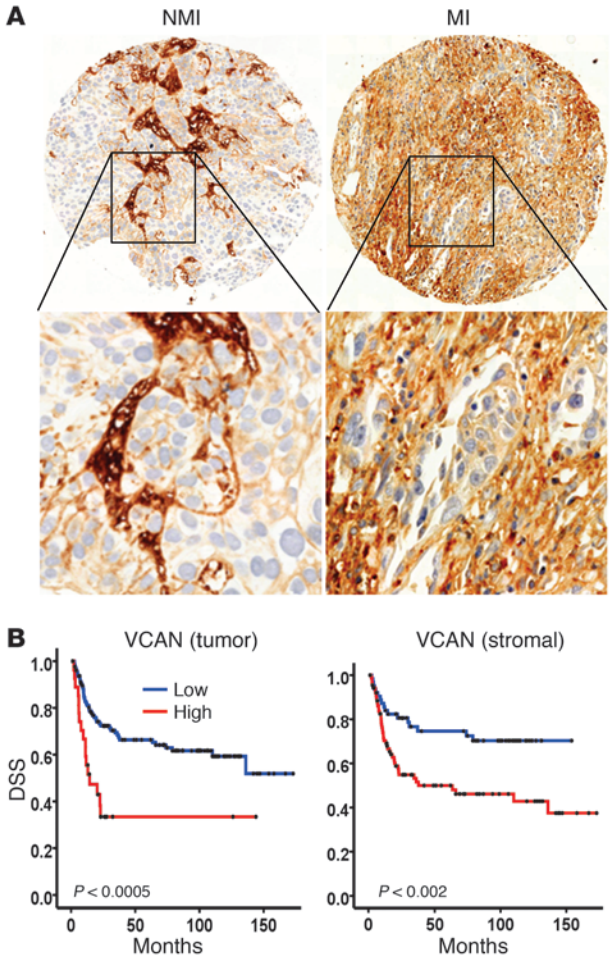

Figure 2
The expression of VCAN in human bladder tumors. (**A**) Immunohistochemical staining and scoring of VCAN in NMI (n = 92) and MI (n = 102) tumors. Original magnification, ×100 (upper panels); ×200 (lower panels). (**B**) Kaplan-Meier plots showing stratification of DSS for all patients as a function of tumor cytoplasmic VCAN (left) and intensity stromal VCAN (right) staining (log rank, $P < 0.0005$ and $P = 0.002$, respectively).

can expression in vivo, we found an anticorrelation (rho –0.274, $P = 0.009$) between GDI2 and VCAN mRNA expression in a completely separate cohort of human bladder tumors (44).

Also consistent with the notion that versican might mediate part of the GDI2 invasion and metastasis suppressor phenotype, we found, in 4 separate microarray cohorts of UCs (44–47), significantly higher RNA expression of versican in MI as compared with non–muscle invasive (NMI) UCs (Figure 1C). In 2 of these cohorts (44, 46), where survival follow-up data was available, we found a significant association between level of expression of versican and survival (Figure 1D). Importantly, expression of versican protein in both tumor cells and stroma of human urothelial carcinoma tissues (Figure 2A) was correlated with poor disease-specific survival (DSS) (Figure 2B).

Lung metastasis and versican expression in vivo are reduced by tumor GDI2. Expression of GDI2 in UMUC3 significantly suppressed the expression of V1, V2, and V3 versican isoforms at the level of transcript, total cellular protein, and protein secretion in conditioned medium (CM) (Figure 3, A and B). In lung colonization assays, GDI2 reexpression in UMUC3 reduced colonization (Figure 3C) and the number of visible lung metastases (Figure 3D) and decreased the expression of V1, V2, and V3 versican isoforms in lung metastatic deposits (Figure 3E).

We (48) and others (49) have reported that pulmonary macrophage infiltration is a prerequisite for lung metastasis development after tail-vein injection of cancer cells. Since versican is a component of the tumor inflammatory response facilitating lung metastases (50) and has been linked to macrophage-mediated inflammatory vascular disease (9, 10, 12, 14, 29, 38, 51–54), we hypothesized that GDI2 might suppress lung metastasis through downregulation of versican, in turn leading to a reduction of macrophage lung infiltration. We compared macrophage infiltration within and adjacent to metastatic lung foci that developed after tail-vein injection of GFP and GDI2 cells and found a reduction in mice injected with GDI2 cells compared with GFP controls (Figure 4A). Additionally, the levels of tumor- and host-derived cytokines (human and murine hIL-6 and hCCL2, mIL-6, and mCCL2) and Cox-2 activity, all implicated in macrophage recruitment, polarization, and inflammation, were decreased in lysates of GDI2-injected lungs (Figure 4, B and C).

Tumor GDI2 reduces versican expression in cancer cell–macrophage cocultures. Versican is regulated by cytokines and other soluble factors in the tumor microenvironment (50). Hence, it is conceivable that cytokines expressed by macrophages in the tumor microenvironment can stimulate their own as well as tumor versican expression. We sought to determine the impact of tumor GDI2 on this process by using a coculture system of cancer cells and U937 macrophages to determine whether such interaction led to alterations in versican expression. Coculture of UMUC3 cells with U937 cells, without cell-cell contact, increased the expression of versican isoforms at the protein (Figure 5A) and transcript levels (Figure 5B) in both cell types, while expression of GDI2 in cancer cells reduced versican induction in both cell types. These findings suggest tumor GDI2 reduces expression of versican in cancer cells and also exerts an effect on macrophage versican expression through cancer cell–secreted factors.

Coculture of cancer cells with primary macrophages or macrophage cell lines induces an increase in proinflammatory cytokines in their CM (48, 55, 56). To determine whether GDI2 regulates this process, we evaluated the effect of GDI2 on inflammatory mediators in coculture, finding that GDI2 expression in cancer cells decreased the secretion of IL-6 and CCL2 cytokines in CM of the cocultures (Figure 5C) as well as Cox-2 activity (Figure 5D). We found a correlation between the expression of versican and the other 2 cytokines in the microarray cohort of human bladder tumors; this finding supports the idea that there is a regulatory relationship among IL-6, CCL2, and versican expression operating in the microenvironment of human bladder tumors (CCL2, rho 0.514, $P < 0.001$; IL-6, rho 0.537, $P < 0.001$).

Tumor GDI2 suppresses cancer cell and macrophage invasion via versican. We next determined the effect of GDI2 on cancer cell invasiveness in response to either complete growth medium (CGM) or U937 macrophages and the role versican played in this process. Knockdown of all versican isoforms in UMUC3 (Figure 6A) phenocopied the antiinvasive profile of GDI2 cells (Figure 6B). Overexpression of V1 and V3, but not V2, isoforms increased UMUC3

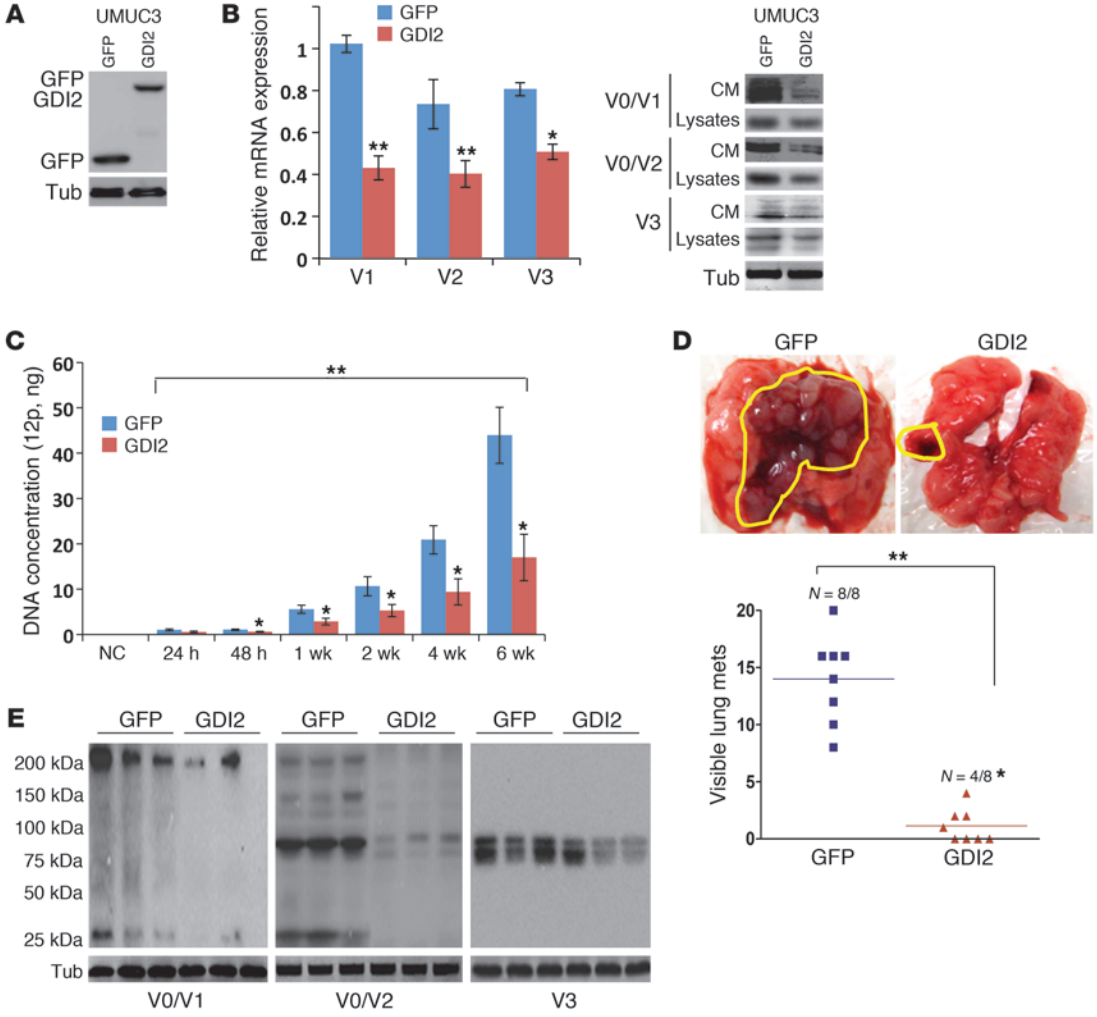

Figure 3

GDI2 overexpression reduces lung metastasis and VCAN expression. (**A**) WBs showing the expression of GFP and GFP in UMUC3 cells. Tub, tubulin. (**B**) The expression of VCAN transcripts (left) and protein (right) in GFP and GDI2 cells was determined by qRT-PCR and WB of cell lysates and CM. Bars represent mean ± SEM, $n = 3$. *$P < 0.05$; **$P < 0.01$ (compared with GFP, Student's t test). Relative expression was normalized to the housekeeping gene GUS-B. Equal protein loading was confirmed by tubulin. (**C**) Tumor cell burden in lungs was determined by qPCR of human 12p chromosome at indicated time points after tail-vein injection of cancer cells. Bars represent mean ± SEM, $n = 3$. *$P < 0.05$, Student's t test, comparing GFP and GDI2. **$P < 0.001$, 1-way ANOVA with Tukey's multiple comparison post-hoc test. (**D**) Photos of lung metastasis (mets) (circled in yellow) and scatter plot of the incidence and number of visible metastases 6 weeks after injection of cancer cells. *$P < 0.05$, χ^2 test, comparing the incidence; **$P < 0.01$, Student's t test, comparing the number of metastases. (**E**) WB of VCAN isoforms in representative lung lysates ($n = 3$) 6 weeks after injection of cancer cells shown in **D**.

matrix invasiveness (Figure 6B) while abrogating the antiinvasive effect of GDI2 reexpression. Since transendothelial migration (TEM) of cancer cells is an important step in metastasis (48, 49), we investigated the effect of GDI2 on cancer cell TEM (48) by evaluating the ability of cancer cells to traverse primary human pulmonary microvascular endothelial cell (PMVEC) monolayers toward either CGM or U937 macrophages. Tumor GDI2 reexpression decreased the cancer cells' ability to traverse PMVECs whether in the presence of CGM or U937 macrophages (Supplemental Figure 1A; supplemental material available online with this article; doi:10.1172/JCI61392DS1). Knockdown of versican phenocopied the inhibitory effect of GDI2 on UMUC3 TEM. V1 and V3 overexpression dramatically increased TEM of GFP cells toward CGM (Supplemental Figure 1A) and U937 cells (Supplemental Figure 1A) as compared with controls and abrogated the inhibitory effect of GDI2 reexpression. In contrast, overexpression of V2 isoform in cancer cells had neither effect. Since cancer cells can exert a chemotactic effect on macrophages (55, 57–61), we investigated the effect of tumor GDI2 on the ability of cancer cells to promote macrophage chemotaxis through Matrigel or PMVECs and found that GDI2 reexpression reduced U937 cell migration compared with GFP controls (Supplemental Figure 1B). Versican depletion in tumor cells had similar effects, while V1 and V3 (but not V2) isoform expression in cancer cells increased their ability to attract U937 cells (Supplemental Figure 1C) and also negated the suppressor effect of GDI2 on U937 chemotaxis.

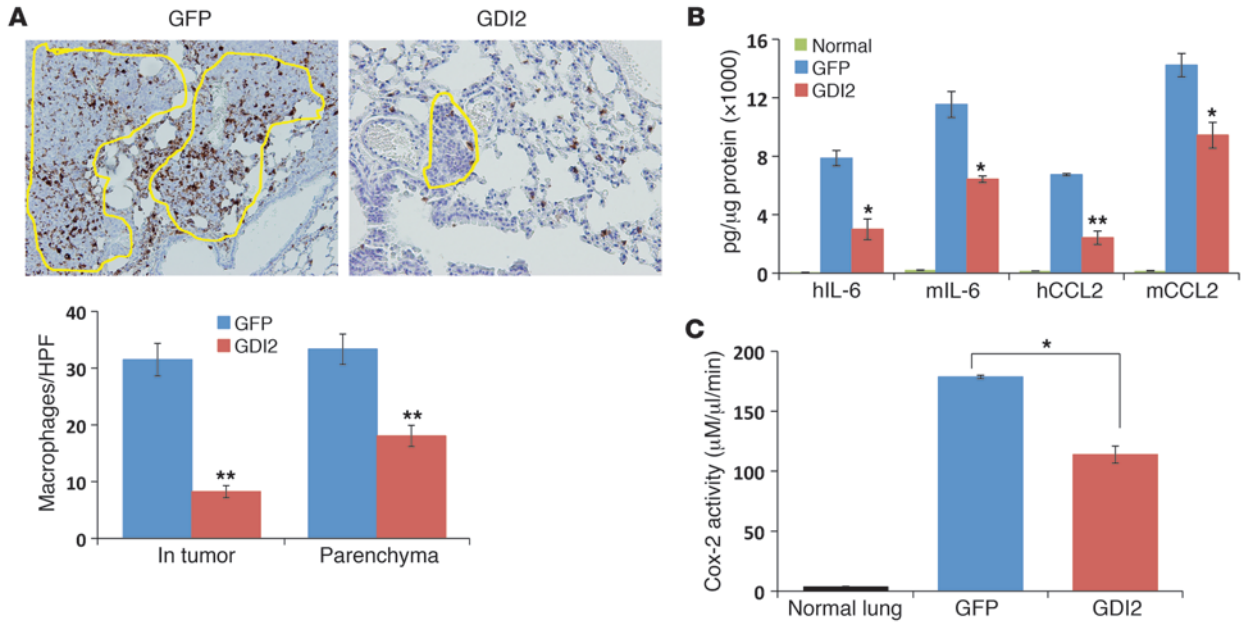

Figure 4

GDI2-reduced lung metastases are associated with decreased lung inflammation. (**A**) Mac2 immunostaining showing macrophage infiltration in lung metastatic foci (circled in yellow) and the surrounding lung parenchyma. Bars represent mean ± SEM of macrophages counted in 6 random fields. $^{**}P < 0.01$, Student's *t* test. Original magnification, ×200. (**B** and **C**) Human IL-6 (hIL-6), CCL2 (hCCL2), murine IL-6 (mIL-6), and CCL2 (mCCL2), and Cox-2 activity were determined in lung lysates. Bars represent mean ± SEM. $n = 3$, performed in duplicate. $^{*}P < 0.05$; $^{**}P < 0.01$, Student's *t* test. HPF, high-powered field.

We next sought to determine whether these findings generalize to other human bladder cancer cell lines and have carried out additional experiments with the human bladder cancer cell lines in which GDI2 was originally identified as a metastasis suppressor (1): T24 (non-metastatic, high GDI2) and T24T (metastatic, low GDI2). Genetic manipulation of V1 and V3 versican by overexpression and depletion in T24 and T24T, respectively (Supplemental Figure 2, A–C), confirmed the results retrieved in the UMUC3 cell line (Supplemental Figure 3, A–C). Together, these results indicate that tumor GDI2, through regulation of V1 and V3 versican isoforms, reduces the ability of cancer cells and macrophages to invade matrix and PMVECs.

Versican is required for metastatic colonization of the lung. Based on the above observations, we hypothesized that GDI2-mediated suppression of metastasis depended on reduction of versican. To test this hypothesis, we compared shVCAN-transduced cells depleted of all isoforms (Figure 6A) with NTsh controls in tail-vein experimental metastasis assays, and found a significant decrease in the incidence and number of lung metastases (Figure 7A). Decreased versican protein expression was confirmed for shVCAN lung lysates and was associated with decreased macrophage infiltration and inflammatory mediators in tumor-bearing lungs (Figure 7, B–D). Knockdown of versican in another metastatic bladder cancer cell line, T24T with low GDI2 expression (ref. 1 and Supplemental Figure 2, A and B), revealed similar results (incidence and number of visible lung metastases after tail-vein injection of T24T-NTsh controls and T24T-shVCAN) (Supplemental Figure 4A). In addition, the levels of versican V1 and V3 protein expression in the lungs as well as macrophage infiltration and proinflammatory mediators were similarly suppressed after knockdown of versican in T24T cells (Supplemental Figure 4, B–D).

To determine whether suppression of versican expression is required for the metastasis suppressor effect of GDI2, we evaluated the effect of ectopic expression of V1 and V3 isoforms in GFP and GDI2 cells on the development of lung metastases. We found that overexpression of V1 and V3 (Figure 8, A and B) in GFP cells was associated with an increase in the incidence, number, and size of lung metastases as compared with their controls (vehicle control [VC]). V1 and V3 overexpression was associated with increased macrophage infiltration (Figure 8, C and D) and V1 and V3 protein expression (Figure 9A) as well as tumor and host inflammatory mediators in tumor-bearing lungs (Figure 9B). Importantly, reconstitution of V1 and V3 levels in cells expressing GDI2 to those found in control cells abrogated the suppressor effect of GDI2 on lung metastases, macrophage infiltration, and inflammatory mediators in tumor-bearing lungs (Figures 7–9). These results support a central role for tumor-derived V1 and V3 versican isoforms in the lung metastasis suppressor effect of GDI2.

Functional blockade of CCL2/CCR2 axis antagonizes versican-mediated lung metastasis. Reports implicate CCL2 in cancer progression and metastasis through their effects on macrophages (49, 58, 62, 63). CCL2 and versican expression are also induced by common factors in vitro (9, 10, 18, 32). Since our results indicate that both human and murine versican and CCL2 in the lung are reduced as a function of tumor GDI2 expression (Figure 4B and Figure 7D), we wondered whether the prometastatic effects of versican require CCL2. We used 2 approaches to answer this. First, we used a syngeneic experimental metastasis assay and the MB49 murine bladder cancer cell line (48) in CCL2 ($Ccl2^{-/-}$) or CCL2 receptor ($Ccr2^{-/-}$) knockout mice and their C57B6/J6 WT counterparts (12, 26, 64). Second, we used both neutralizing antibody

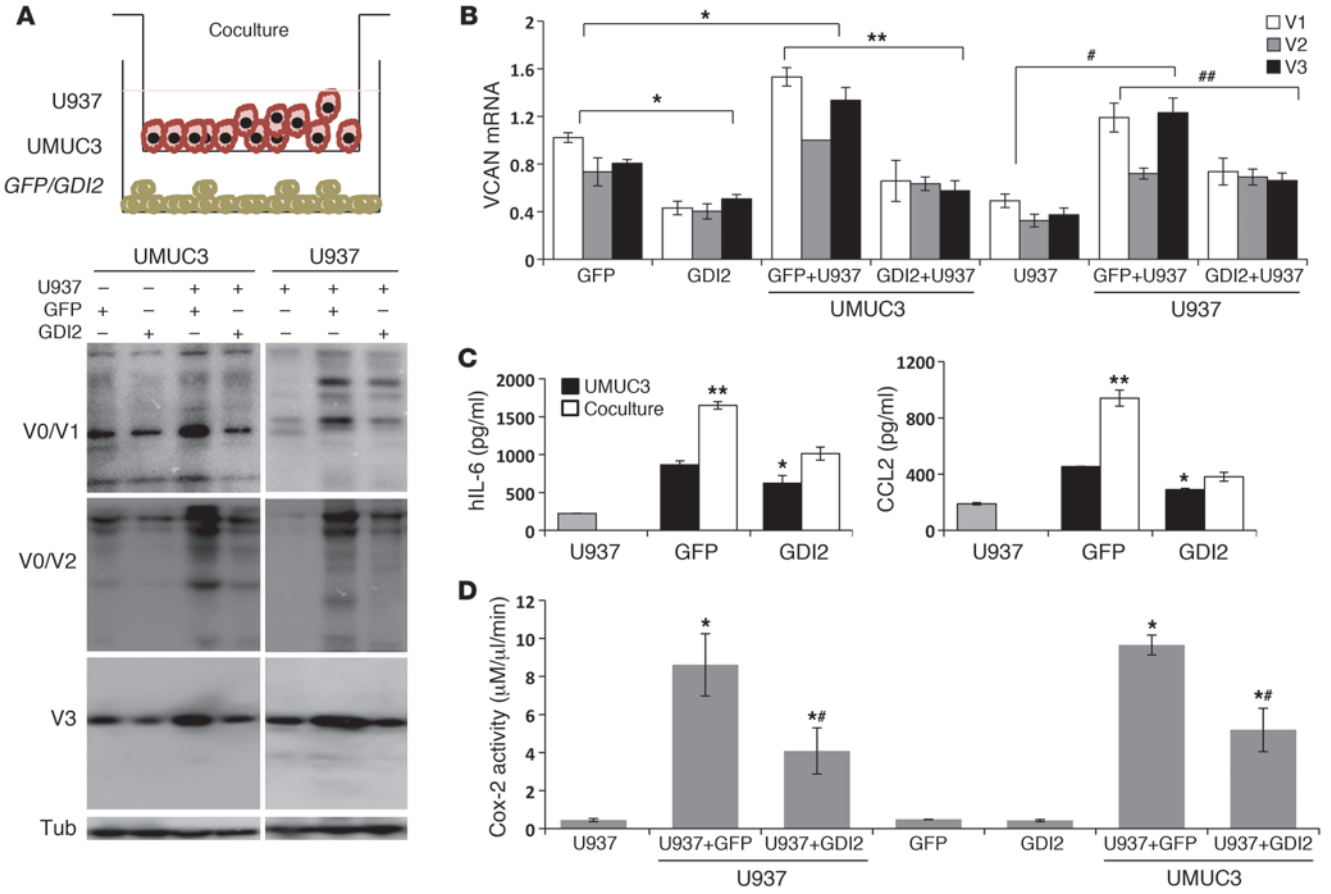

Figure 5

GDI2 modulates cancer cell–macrophage interactions through VCAN. (**A**) Schema of UMUC3-U937 cocultures. WB showing the expression of VCAN isoforms in UMUC3 or U937 lysates cocultured for 72 hours. (**B**) qRT-PCR (after 6 hours) in cell lines under the same conditions as in panel **A**. In all coculture experiments, bars represent evaluated cells (U937 or UMUC3) that appear below the lines in the *x* axis labels. $^{*}P < 0.01$, compared with GFP in single-cell culture; $^{**}P < 0.01$, comparing GFP and GDI2 in cocultures; $^{\#}P < 0.05$, comparing U937 in single and cocultures; $^{\#\#}P < 0.05$, comparing U937 cocultured with GFP and GDI2. (**C**) hIL-6 and hCCL2 in 72-hour CM of single cultures of U937 (gray bars) or UMUC3 (either GFP or GDI2, black bars) and in cocultures of U937 with UMUC3 (either GFP or GDI2, white bars). $^{*}P < 0.05$, comparing GFP and GDI2; $^{**}P < 0.01$, comparing single cell to coculture. (**D**) Cox-2 activity was determined in cell lysates under the same conditions as in **A**. $^{*}P < 0.01$, comparing single cells to cocultures; $^{\#}P < 0.01$, comparing cocultures with GFP versus GDI2. Student's *t* test was used.

to CCL2 (65) and an antagonist to CCR2, RS102895 (66, 67), in experimental metastasis assays using V1 and V3 versican isoform–overexpressing UMUC3 cells.

We found significantly reduced lung metastasis (Figure 10A) and macrophage infiltration in the lung (Figure 10B) following MB49 tail-vein injection in *Ccl2*$^{-/-}$ and *Ccr2*$^{-/-}$ mice. The lack of host CCL2, but not CCR2, was associated with decreased expression of V1, but not V2, murine versican isoforms (no anti-V3–specific murine antibody was available) (Figure 10C), yet both were associated with a decrease in IL-6 and CCL2 (Figure 10D). We also found that functional blockade of CCR2 by RS102895 significantly reduced the incidence and number of lung metastases of UMUC3-GFP cells at baseline and upon overexpression of V1 and V3 (Figure 10E); this finding supports the importance of CCL2. Use of an antibody to neutralize CCL2 resulted in a similar reduction in metastases of UMUC3 cells at baseline and with overexpression of versican isoforms V1 and V3 (Figure 10F). These results indicate that the CCL2 and CCR2 are important in GDI2-versican–mediated lung metastasis in both murine and human models of disease.

Macrophage depletion inhibits versican-driven lung metastasis. Our findings that the metastasis suppressor effect of GDI2 is mediated through modulating cancer cell–macrophage interactions and downregulation of versican prompted us to investigate whether macrophage recruitment contributes to versican-mediated metastasis. First, we transiently ablated macrophages by administration of clodronate liposomes (48–50) and found that pharmacologic ablation of macrophages not only decreased the incidence, number, and size of UMUC3-GFP lung metastasis, but also mitigated metastasis induced by overexpression of V1 and V3 (Figure 11A and Figure 12A). Interestingly, clodronate did not further reduce lung metastasis or macrophage infiltration in UMUC3-GDI2 cells, while macrophage infiltration of the lungs and metastasis was significantly suppressed by clodronate treatment of UMUC3-GFP (Figure 11B and Figure 12B). The expression levels of host and tumor IL-6 and CCL2 as well as Cox-2 activity in tumor-bearing lungs were significantly decreased after clodronate treatment (Figure 11, C and D, and Figure 12, C and D). Taken together, these data argue that macrophage infiltration in the lung plays a central

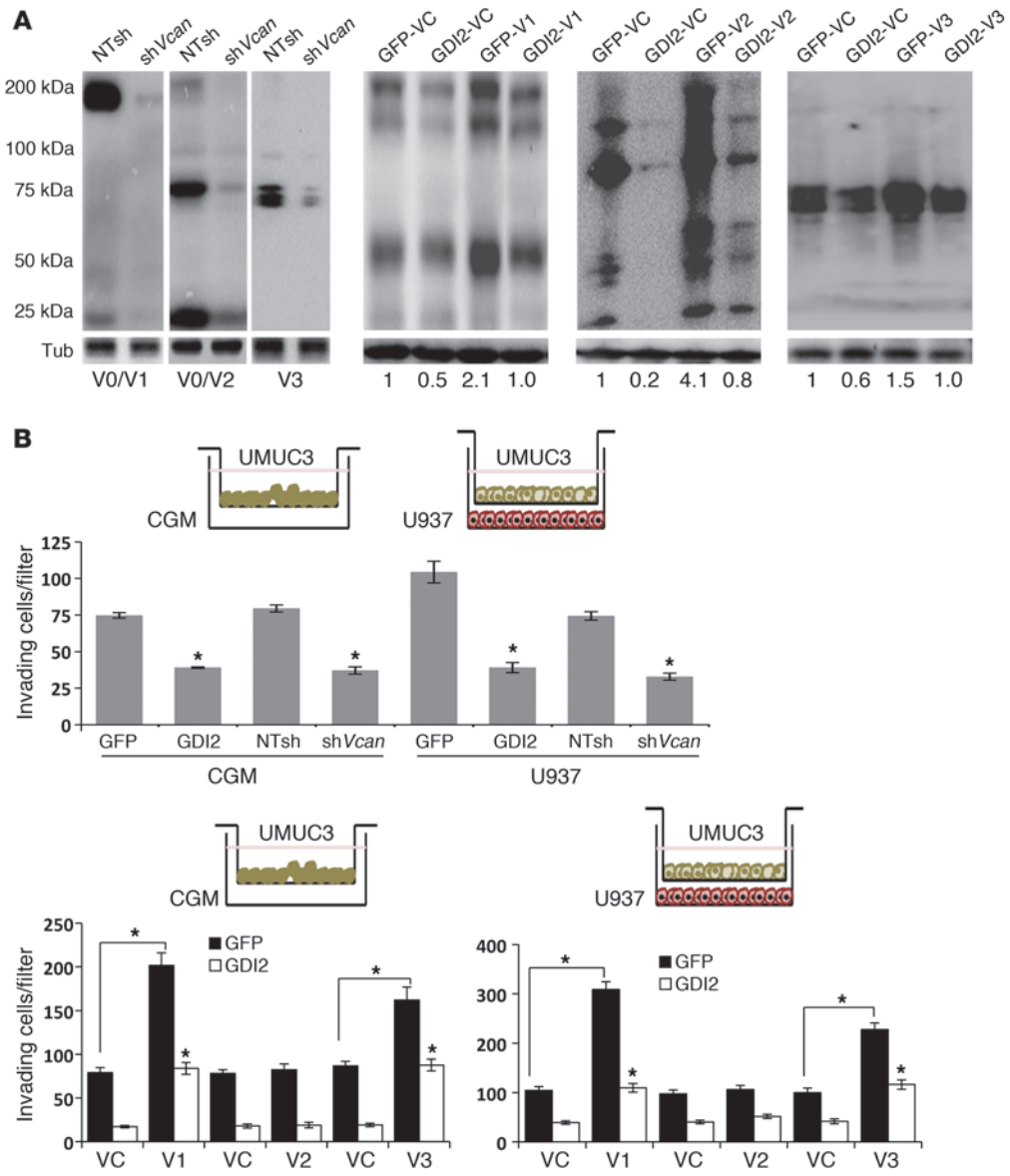

Figure 6
Effect of genetic manipulation of VCAN in UMUC3 cells on their in vitro appearance. (**A**) WB confirming the efficiency of *Vcan* knockdown/expression in UMUC3-GFP and UMUC3-GDI2 cells transduced with shRNA lentiviruses targeting all VCAN isoforms (sh*Vcan*), an irrelevant nontarget (NTsh), or retroviruses overexpressing V1, V3, and V2 and their empty vector controls (VC). Numbers represent the relative band density normalized to corresponding tubulin, with GFP-VC considered as 1. (**B**) Engineered UMUC3 cells in **A** were allowed to invade Matrigel-coated 8-μm inserts toward CGM or U937. $^*P < 0.05$. Bars represent mean ± SEM of counted invading/attracted cells of 3 independent experiments performed in triplicate. Student's *t* test was used.

role in GDI2-mediated metastasis suppression via downregulation of V1 and V3 versican isoforms.

Discussion

Clinical data from human disease as well as experimental rodent models of carcinogenesis and metastasis reveal that bladder cancer primarily metastasizes to the regional lymph nodes and the lungs. (68). The high incidence of pulmonary metastases in cancer patients was initially believed to be a random process; however, recent reports indicated that the development of lung metastasis is likely an active highly selective process instigated by tumor cells and strongly influenced by their interactions with host cells present in the tumor microenvironment (69). Given that metastases are responsible for most of the deaths from this disease, understanding of this process is critical.

Using common patterns of gene expression between bladder cancer models and cohorts of human bladder tumors, we inferred a possible linkage between reduced GDI2 expression and high expression of the ECM molecule versican and poor clinical outcomes. Specifically, the relationship of expression of versican and GDI2 to patient survival, together with empiric observation of repression of versican by reexpression of GDI2 in bladder cancer cell lines suggested that its metastasis suppressor function may depend on a reduction of versican. Herein we report that the primary mode of action of the metastasis suppressor molecule GDI2 is via reduction of the tumor-promoting inflammatory response that has recently emerged as the seventh hallmark of cancer (70). We used complementary pharmacologic and genetic preclinical models and tools in vitro and in vivo to provide a mechanistic link between the observed clinical associations of GDI2 to versican and demonstrated the causal relation between the GDI2 suppression of metastasis and reduction of versican V1 and V3 isoform expression in several models of human bladder cancer.

Versican is a complex and versatile ECM molecule that is indispensable for life (8, 29). It functions not only as a scaffold or substrate to be consumed during tumor-cell invasion, but represents a

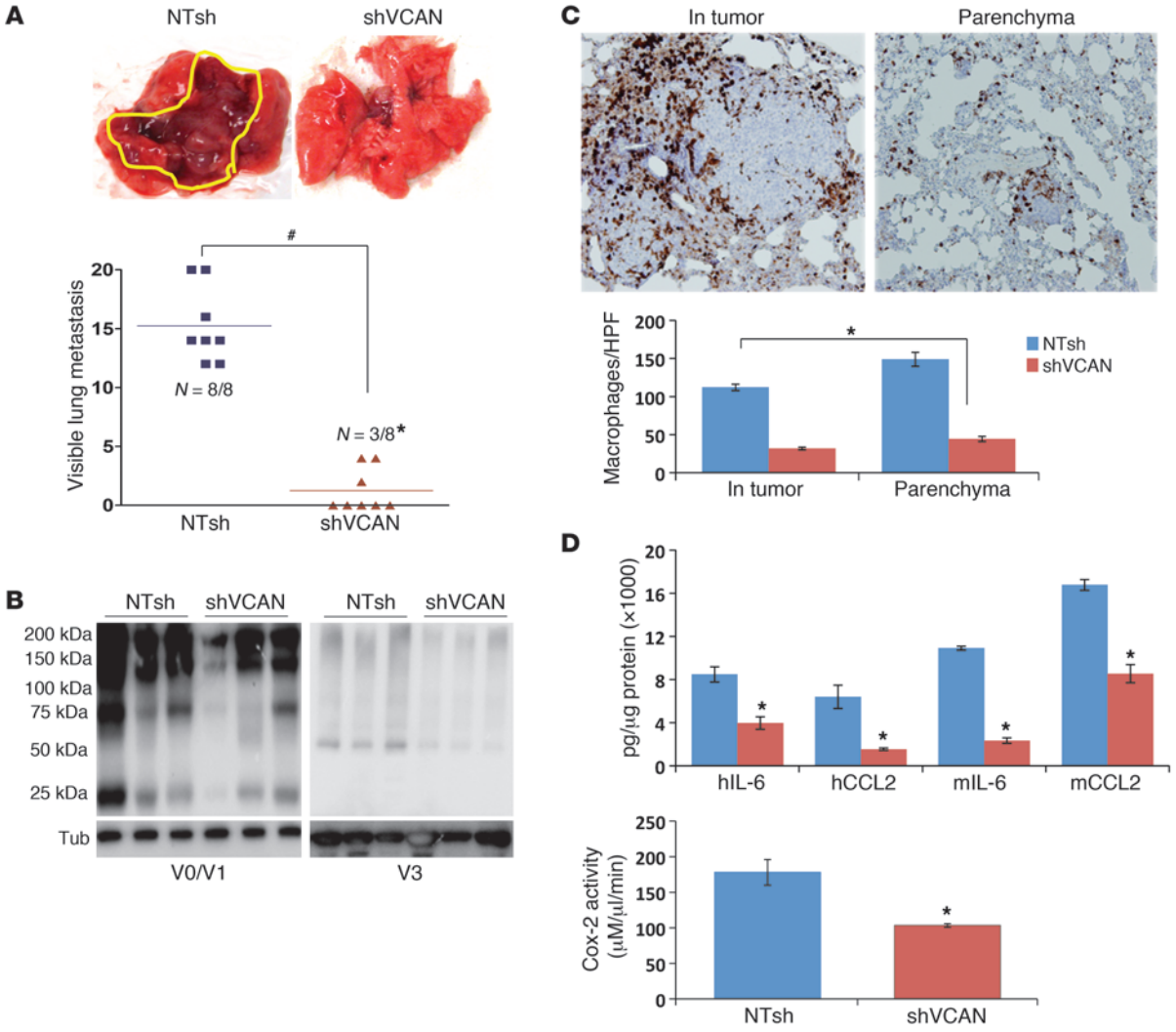

Figure 7

VCAN expression is necessary for lung metastasis. (**A**) Photos of lung metastasis (circled in yellow) and scatter plots showing the incidence and number of visible lung metastases 6 weeks after tail-vein injection of UMUC3-sh*Vcan* and NTsh controls. $^{*}P < 0.01$, χ^2 test comparing incidence; $^{\#}P < 0.01$, Student's *t* test, comparing the number of visible lung metastases. (**B**) The expression of VCAN isoforms in lung lysates was determined by WB at 6 weeks after inoculation in samples from **A**. (**C**) The number of macrophages is shown and counted as described in Methods. Bars represent mean ± SEM of the number of macrophages (6 random fields). Original magnification, ×200. $^{*}P < 0.05$, Student's *t* test. (**D**) hIL-6, hCCL2, mIL-6, and mCCL2 levels and Cox-2 activity in lung lysates. Bars represent mean ± SEM ($n = 3$, performed in duplicate). $^{*}P < 0.05$, Student's *t* test.

central component of cancer-related inflammation, as it can bind multiple types of cell adhesion receptors, growth factor receptors, and chemokines to provide a complex set of environmental cues to inflammatory and cancer cells in versican-rich sites (21, 29, 71). Our work demonstrated an association between the expression of GDI2, versican, and inflammatory cytokines such as CCL2 and revealed that CCL2 chemokine expression was a key determinant of tumor versican-driven metastasis. Several reports have implicated this chemokine in myriad activities that have an impact on cancer progression and metastasis (49). Tumor CCL2 has been implicated in recruiting $CCR2^{+}$ myeloid cells not only to primary tumor, but also to prospective metastatic sites, promoting their maturation and differentiation into an inflammatory phenotype that fosters extravasation, seeding, and persistent growth of tumor cells (49, 56, 63, 72–76). Indeed, recent data demonstrate that targeting CCL2 with antibodies inhibited lung and bone metastases in vivo and may represent a novel approach to cancer treatment (49, 63, 76). However, until our report, it had not, to our knowledge, been reported that host CCL2 is necessary for versican-driven metastasis, allowing possible patient stratification. CCL2 transcription as well as the signaling pathways triggered by the CCL2/CCR2 axis have been shown in various systems to be regulated by NF-κB, and AP-1 either directly or through other signaling intermediates (63, 65, 72, 73, 75–79). Thus, one could speculate that factors in the tumor microenvironment that trigger these signaling intermediates could induce both versican and CCL2. Given that versican promotion of metastasis is dependent on host CCL2, such parallel induction would confer an advantage to a tumor by maximally promoting metastatic colonization.

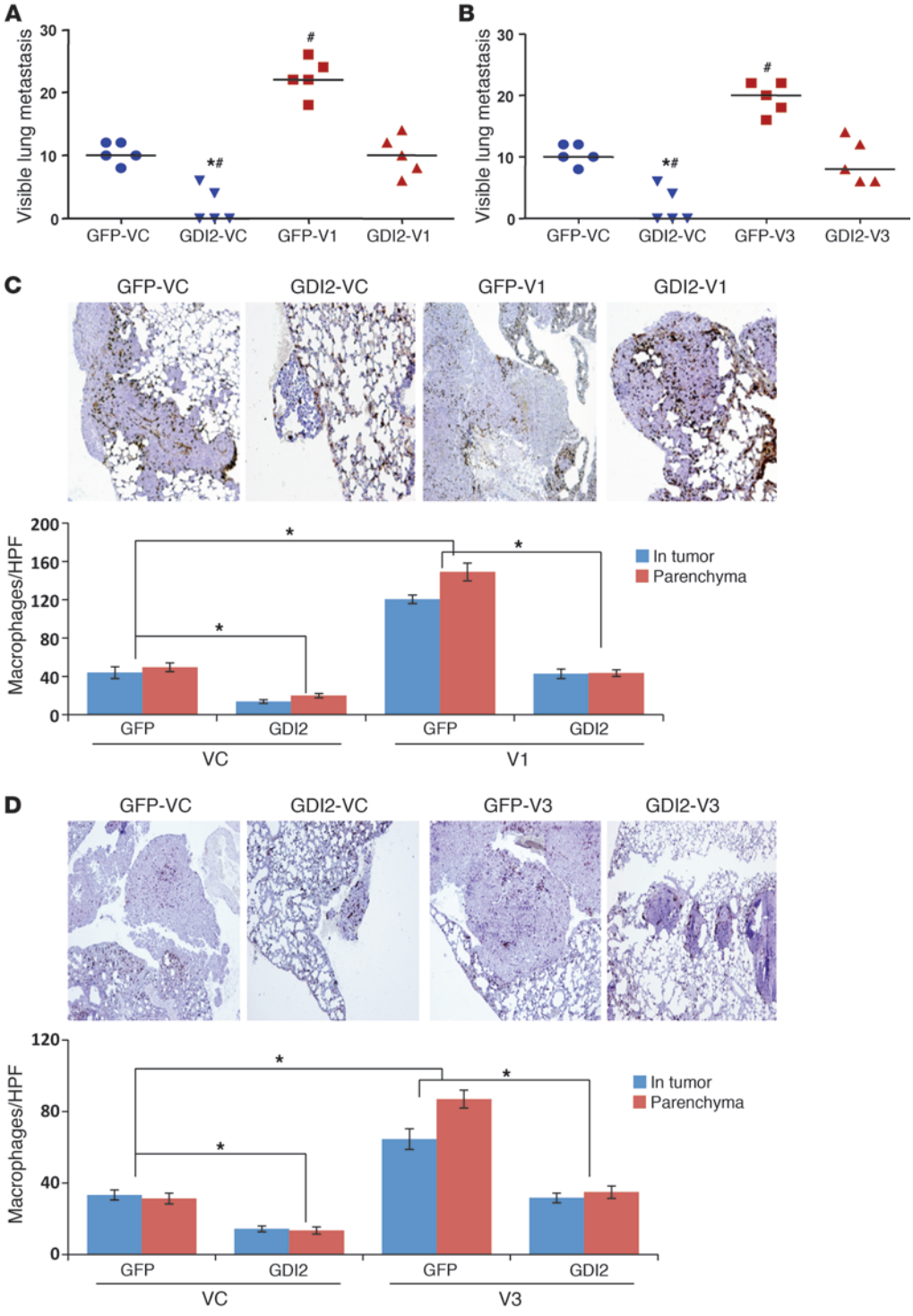

Figure 8
Reexpression of V1 and V3 VCAN mitigates RGDI2 metastasis suppressor effect. (**A** and **B**) Scatter plots showing the incidence of number of lung metastases after reexpression of V1 and V3 in GFP and GDI2 cells. $^{*}P < 0.01$, χ^2 test comparing the incidence; $^{\#}P < 0.01$, Student's *t* test, comparing the number of visible metastases. (**C** and **D**) The number of macrophages in the lungs corresponding to samples shown in **A** and **B** counted as described in Methods. Bars represent mean ± SEM of the number of macrophages/HPF. $^{*}P < 0.05$, Student's *t* test.

The association of GDI2 expression and metastasis development appears to be tumor-type dependent. The metastasis suppressor effect of GDI2 in bladder cancer has been shown to be influenced by its unconventional regulation of RhoGTPases and posttranscriptional modification (42, 80). Interestingly, in other tumors where this protein has been studied, such as breast (46, 81) and colon cancer (82), its levels have been directly associated with worse patient prognosis. While the mechanisms of action of GDI2 in these cancers have not been fully elucidated, it is conceivable that the interactions of GDI2 with its downstream effectors are influenced by the tumors' histological type. If indeed the hypothesis that the versican-CCL2-macrophage axis we describe here is critical for metastasis in multiple tumor types, one would expect that in these cancers, the expression of GDI2 would be directly related to that of versican as opposed to being inversely related as we found in bladder tumors. Preliminary data has shown that this is indeed the case (Y. Ru and D. Theodorescu, unpublished observations). The importance of this finding is that it provides us with tools to dissect the

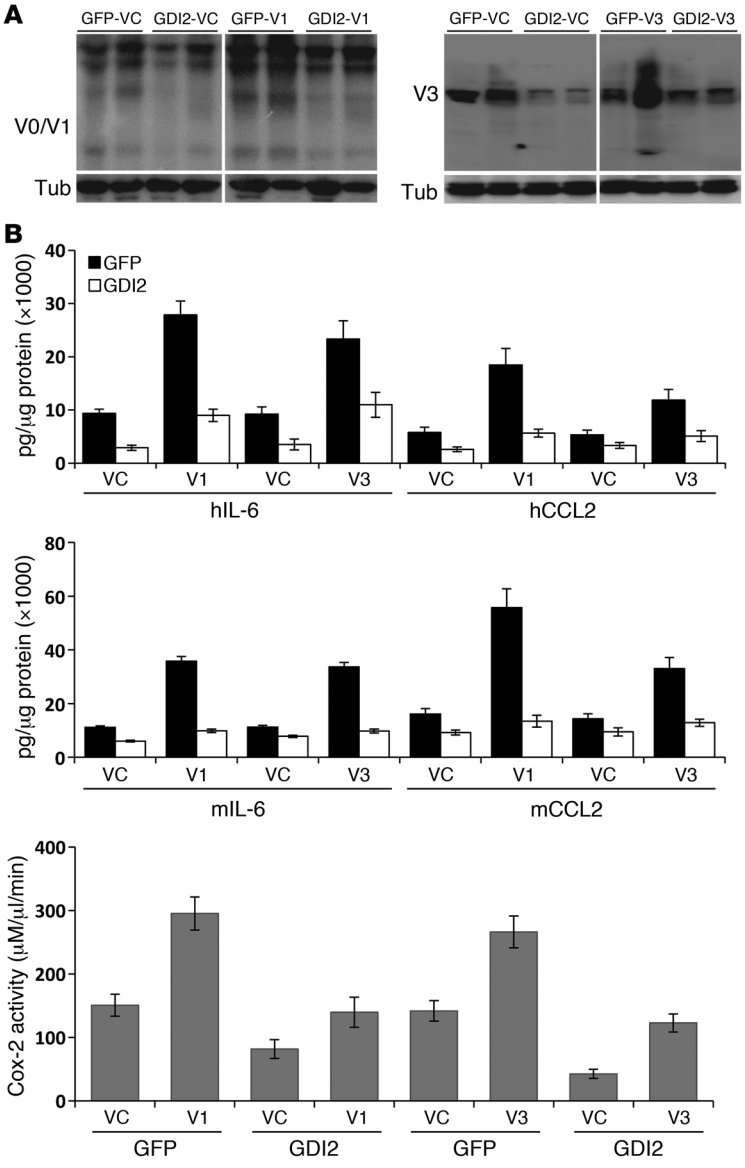

Figure 9
Forced expression of V1 and V3 in GFP and GD12 cells increased lung VCAN and inflammatory mediators. (**A**) WB showing the expression of VCAN isoforms in metastasis-bearing lungs. (**B**) hIL-6, hCCL2, mIL-6, and mCCL2 levels and Cox-2 activity in lung lysates. Bars represent mean ± SEM (n = 3, performed in duplicate).

tumor-type dependent pro- and antimetastatic effects of GDI2, which has previously been an intractable biological problem.

In conclusion, considering that versican is important for outgrowth of disseminated cancer cells, therapeutically targeting versican or blocking the cytokines required for its function, such as CCL2, may provide a strategy for delaying the evolution of clinical metastatic disease from microscopic deposits. Use of specific antibodies or small molecule antagonists against the CCR2 appears to be a promising anticancer strategy that can be specifically targeted at high-versican–expressing tumors, optimizing the chance for clinical response.

Methods

Cell culture, plasmids, transfections, and viral transductions

Human UMUC3, T24, T24T, human monocytoid U937, and murine MB49 cells were obtained from and maintained as recommended by ATCC. PMVECs were obtained from and maintained as recommended by Lonza. UMUC3 cells stably expressing GDI2 tagged by pEGFP-C1 were generated as earlier described (42). Stable knockdown of all versican isoforms was done using shRNAs V1 5′-CCGGGC-CACAGTTATTCCAGAGATTCTCGAGAATCTCTGGAATA-ACTGTGGCTTTTTG-3′ or nontarget shRNA (NTsh) control vector, cloned in pLKO.1-puro (Mission-TRC; Sigma-Aldrich) following the manufacturer's protocol. shRNA plasmids were packaged in 293T cells by cotransfection with compatible packaging plasmids (Adgene). Culture supernatants containing the viral particles were collected 48 hours after transfection and filtered through 0.45-μm filters (Thermo Fisher Scientific). UMUC3, T24, and T24T cells were transduced with lentivirus-containing supernatant in the presence of 8 μg/ml polybrene (Sigma-Aldrich) for 24 hours. Virus-containing medium was replaced with selection medium containing 1 μg/ml puromycin (Sigma-Aldrich) for 2 weeks. Cells with the most efficient knockdown were used in subsequent experiments. Human V1 vector (5, 83), originally developed by Deiter Zimmermann (University of Zurich, Zurich, Switzerland), was cloned in a retroviral vector (50) and was a gift from Michael Karin (UCSD, San Diego, California, USA), with the permission of Deiter Zimmermann. V3 retroviral vector (52) and V3 overexpression vector were gifts of Thomas Wight (Hope Heart Matrix Biology Program, Benaroya Research Institute at Virginia Mason, Seattle, Washington, USA). V2 expression vector was a gift of Burton Yang (University of Toronto, Toronto, Ontario, Canada). Plasmid transfection, viral transduction, and antibiotic selection of stable cell lines were carried out as described earlier (50, 52, 84, 85).

In vivo experiments

Female athymic (nu^+/nu^+) mice, 4 to 6 weeks of age (National Cancer Institute), were treated following the approved guidelines of the Animal Care and Use Committee of the University of Virginia. For experimental metastasis, cancer cells were injected in the lateral tail vein (48). Mice were euthanized at indicated time points after injection when lungs were harvested, and the number of visible surface metastases was counted. Tissues were either processed for immunohistochemistry (IHC) or snap-frozen for molecular analyses (48). For therapeutic experiments, mice were randomized into groups that received clodronate encapsulated in liposome nanoparticles (5 mg/ml) or empty liposomes as earlier described (48) before tail-vein injection of cancer cells. For syngeneic metastasis experiments, 5- to 6-week-old *Ccl2*$^{-/-}$ and *Ccr2*$^{-/-}$ mice and their WT counterparts (C57B6/J6) were obtained from Jackson Laboratories and received a tail-vein injection of 1×10^4 MB49 cells/100 μl phenol red–free RPMI 1640. Mice were euthanized after 3 weeks, and lung metastases were enumerated. In some experiments, nude mice were injected with UMUC3 cells overexpressing V1, V2, and V3 human isoforms and were randomized into groups that received neutralizing antibody to human CCL2 (MAB679, R&D Systems) or control mouse IgG (10 μg/mouse) injected intraperitoneally every 4 days from the date of

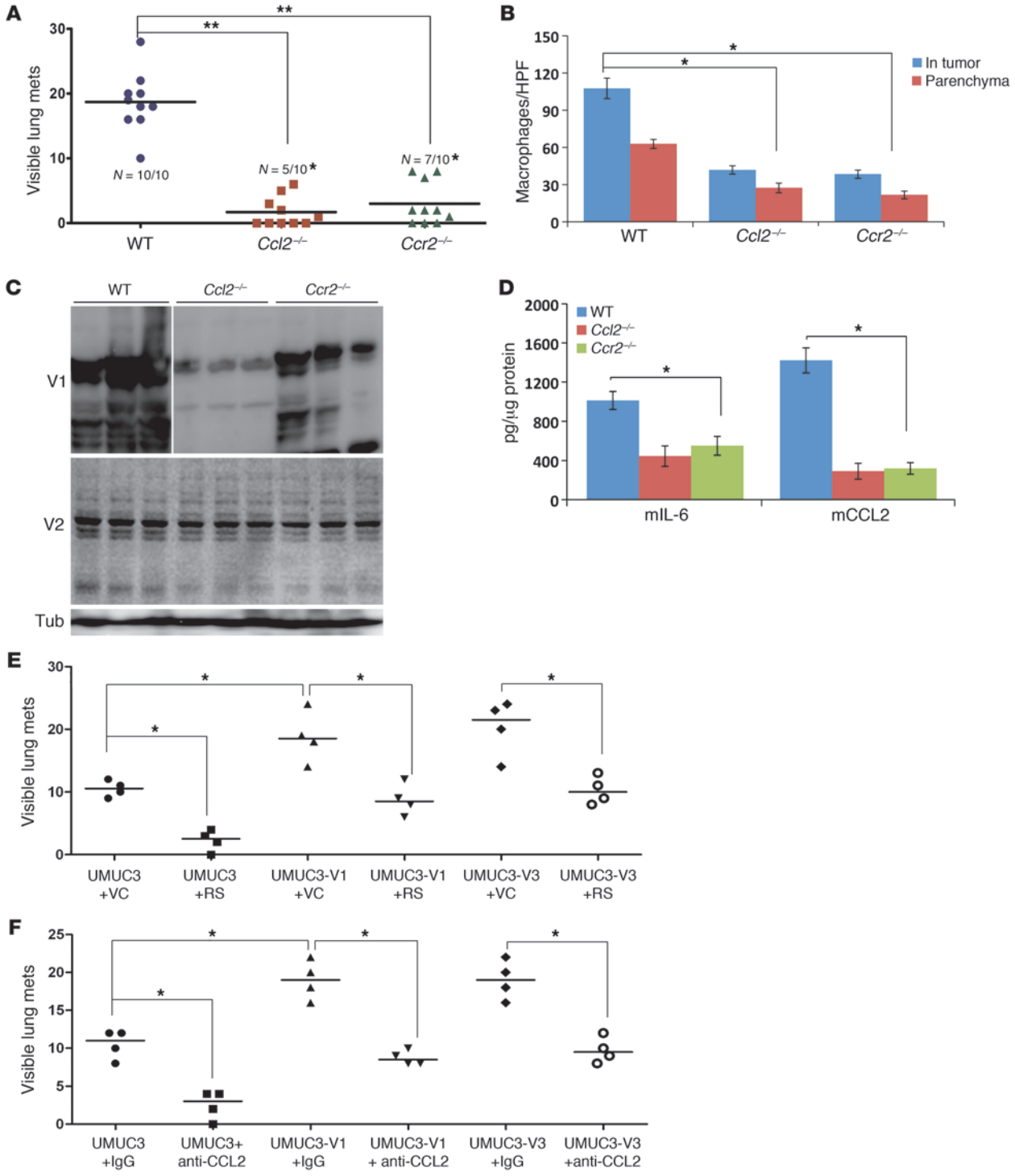

Figure 10

Involvement of CCL2 and CCR2 in VCAN-mediated lung metastasis. (**A**) Scatter plots of the incidence and multiplicity of lung metastases after tail-vein injection of murine MB49 cells (1×10^4 cells/100 μl) in *Ccl2*$^{-/-}$ and *Ccr2*$^{-/-}$ mice and their WT counterparts (WT, C57BL/6). *$P < 0.05$, χ^2 test, comparing the incidence; **$P < 0.01$, Student's *t* test, comparing the number of lung metastases between WT and *Ccl2*$^{-/-}$ aand *Ccr2*$^{-/-}$ cohorts, 3 weeks after injection of tumor cells. (**B**) Mac2 IHC of lung sections of mice in **A**. Bars represent mean ± SEM of the number of macrophages/HPF. *$P < 0.05$, Student's *t* test. (**C**) WB of murine V1 (β-GAG) and V2 (α-GAG) in tumor-bearing lung lysates. (**D**) Murine cytokines in WT, *Ccl2*$^{-/-}$, and *Ccr2*$^{-/-}$ lung lysates. Bars represent the mean ± SEM of 3 independent experiments performed in duplicates. *$P < 0.01$, Student's *t* test. (**E** and **F**) Scatter plots of the incidence and multiplicity of lung metastases developed after tail-vein injection of transfected/transduced UMUC3 cells in nude mice treated with CCR2 antagonist RS 102895 (RS) and its VC or neutralizing antibody against human CCL2 (anti-CCL2) and isotype control IgG. *$P < 0.01$, χ^2 test, comparing the incidence, and Student's *t* test, comparing the number of visible lung metastases.

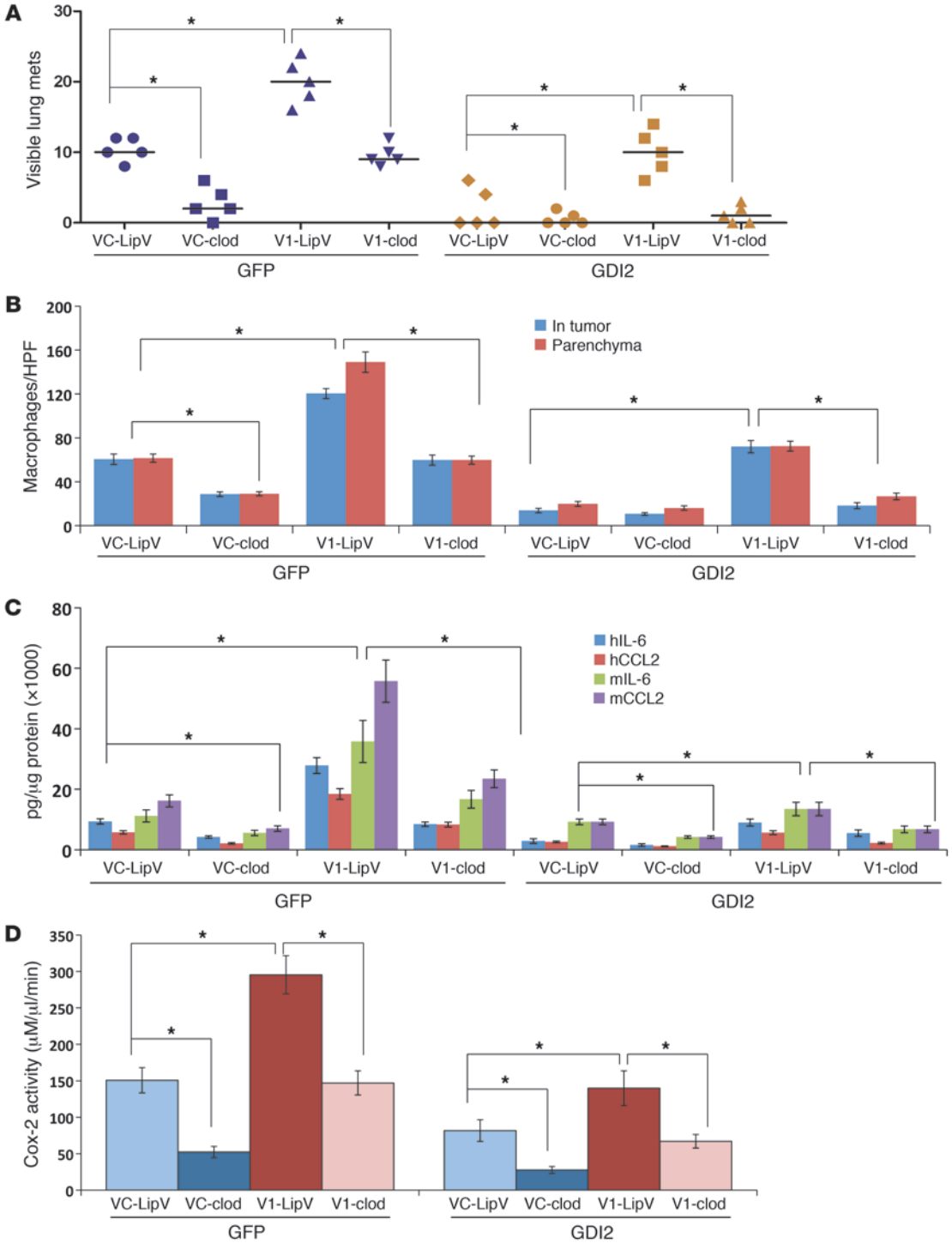

Figure 11

Pharmacologic depletion of macrophages blocks V1-driven lung metastasis and inflammation. (**A**) Plots of incidence and multiplicity of lung metastases after tail-vein injection of V1-expressing GFP and GDI2 cells in nude mice treated with liposome-encapsulated clodronate (clod) or empty liposome vehicle (LipV). (**B**) Bars are mean ± SEM of the number of macrophages infiltrating the lungs/HPF. *$P < 0.05$, Student's *t* test. (**C** and **D**) Human and murine cytokines and Cox-2 activity in lung lysates of mice under the experimental conditions described above. *$P < 0.05$, Student's *t* test.

tumor cell inoculation (65). CCR2b small molecule inhibitor RS102895 was given every 4 days at 10 mg/kg by oral gavage (66, 67). Mice were euthanized 6 weeks after tumor cell injection. Lungs were extracted and the number of visible metastases was quantified.

Quantitative real-time PCR

Tumor cell burden was determined by quantifying human 12p chromosome in genomic DNA in mouse lungs as described previously (48). Versican isoforms were detected in cells and tissues by quantitative RT-PCR

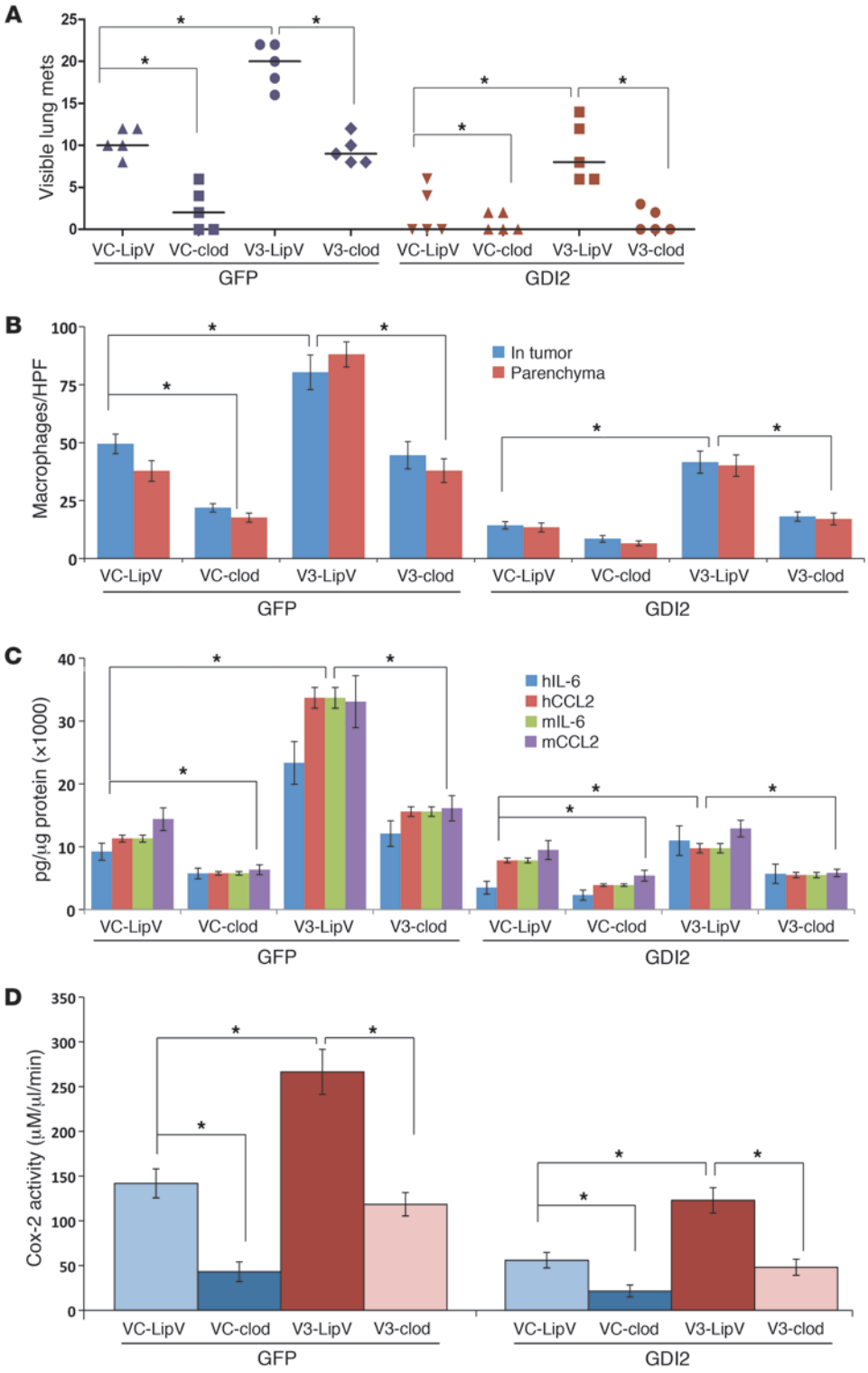

Figure 12
Pharmacologic depletion of macrophages blocks V3-driven lung metastasis and inflammation. (**A**) Scatter plots of the incidence and multiplicity of lung metastases that developed after tail-vein injection of V3-expressing GFP and GDI2 cells in nude mice with and without clodronate treatment. (**B**) Bars represent the mean ± SEM of the number of macrophages infiltrating the lungs/HPF. *$P < 0.05$, Student's *t* test. (**C** and **D**) Human and murine cytokines and Cox-2 activity in lung lysates of mice under the experimental conditions described above. *$P < 0.05$, Student's *t* test.

(qRT-PCR). RNA was isolated using RNeasy Kit (QIAGEN) and reverse transcribed with Superscript III Kit (Invitrogen) according to the manufacturer's instructions. Primers used for amplifying versican isoforms were described earlier (86). qPCR was performed using the SYBR Green PCR Master Mix and Bio-Rad iCycler (Bio-Rad). The relative expression was normalized to the housekeeping gene Gus-B.

Antibodies and Western blots

Human-specific versican antibodies include the following: polyclonal rabbit anti-human V0/V1 and V0/V2 antibodies (Thermo Fisher Scientific). The 12C5 anti-versican antibody, which recognizes the N-terminal domain on V3, was obtained from the Developmental Studies Hybridoma Bank (University of Iowa, Iowa City, Iowa, USA). Rabbit polyclonal anti-

versican antibodies that detect mouse protein include the following: V1 (β-GAG) and V2 (α-GAG) (AbD Serotec). GDI2 antibody was purchased from Spring Bioscience. Mac-2 and F4/80 antibodies were purchased from BD Biosciences and AbD Serotec. Mouse monoclonal antibody against α-tubulin was from Sigma-Aldrich. Monoclonal antibodies against human MCP-1/CCL2 (MAB679) and isotype control IgG were from R&D Systems and Coulter, respectively.

Immunoblotting

Subconfluent monolayers of human bladder cancer cells were grown in 6-well plates, serum-starved in serum-free medium (SFM) overnight, and allowed to condition for 72 hours. In some experiments, cells were cocultured with U937 (1×10^6 cells/ml SFM) and added to 0.4-μm Transwell chambers (Costar; Corning) without direct cell-cell contact. CM was collected and cleared by centrifugation. Cells in upper and lower chambers were harvested in lysis buffer (20 mM Tris, pH 7.4, 150 mM NaCl, 1 mM EDTA, 50 mM NaF, 0.5% sodium deoxycholate, 1% NP-40, 1 mM Na_3VO_4, and 1× protease inhibitor cocktail mixture). Tumor-bearing and control lung tissues were pulverized in lysis buffer and cleared by centrifugation at 12,000 *g* for 20 minutes at 4°C; protein concentrations were determined by bicinchoninic acid (BCA) assay (Pierce; Thermo Fisher Scientific). Cell and tissue lysates and CM were resolved by 4%–20% SDS-PAGE, transferred onto PVDF membranes (Bio-Rad), and probed with the indicated antibodies. For detection of V3 isoforms, cell and tissue lysates were treated in vitro with 0.4 U/ml chondroitinase ABC (ChABC) in 100 mM sodium acetate, pH 8.0, for 1 hour at 37°C, boiled for 10 minutes in reducing denaturing Laemmli buffer, cleared by centrifugation, and subjected to Western blot (WB) using 12C5 anti-versican antibody. Protein detection was carried out using HRP-conjugated secondary antibodies and SuperSignal Femto Maximum Sensitivity Substrate (Pierce).

Microinvasion and TEM assays

Invasion and chemotaxis assays were performed as described previously (48, 56, 78). PMVECs were grown to confluence on 3- and 8 μm-pore filters in 24-well plates, and TEM assays of U937 and cancer cells were carried out as described earlier (48, 56, 78).

Determination of CCL2, IL-6, and Cox-2 activity

Commercial ELISA kits were used to determine the concentrations of human and murine IL-6 and CCL2 (RayBiotech. Inc.). Enzyme immunoassay kits for Cox-2 activity (Cayman Chemical Inc.) were used according to the manufacturer's instructions.

Construction and immunostaining of bladder cancer tissue microarray

Protein expression patterns of versican were assessed using 2 tissue microarrays (TMAs) (87, 88). Antigen-retrieval methods (0.01% citric acid for 15 minutes under microwave treatment) were utilized prior to incubation with mouse anti-versican monoclonal antibody (LifeSpan BioSciences) at 1:400. Staining conditions were optimized on sections from formalin-fixed, paraffin-embedded testis as positive control, as recommended by the manufacturer. The absence of primary antibody was used as a negative control. The secondary antibodies (Vector Laboratories) were biotinylated horse anti-mouse antibodies (1:500 dilution). Diaminobenzidine was utilized as the final chromogen and hematoxylin as the nuclear counterstain (48, 87, 88). The consensus value of the 3 or 4 representative cores from each tumor sample arrayed was used for statistical analyses. Versican expression was evaluated in the tumor and in the stroma. Versican staining in the stroma surrounding the tumor was categorized as negative (–), low (+), intermediate (++), and high (+++). Cutoffs of expression for prognostic evaluation were selected based on the median values of expression among the groups under analysis. For tumor scoring, "high" was designated as staining more than 10% of tumor cells. For stromal versican, the presence of any staining was designated as "high."

Statistics

Human gene-expression profiling data. Duplicate isolates of mRNA from GFP or GDI2 reexpressing UMUC3 cells (42) were profiled for gene expression using Affymetrix HG-U133 Plus 2.0 microarrays as described before (2). Microarray data has been submitted (GEO GSE35014). Normalized $\log_2$ expression values were extracted by RMA implemented in MATLAB version R2010B (MathWorks). For comparison with human tumor cohorts, data sets used included Sanchez-Carbayo et al. (44) (n = 26 and 65, for NMI and MI disease, respectively), Stransky et al. (45) (n = 16 and 14 for NMI and MI disease, respectively), Kim et al., GSE13507 (46) (n = 103 and 62 for NMI and MI disease, respectively), and 2 studies by Dyrskjot et al., GSE3167 and GSE89 (43, 47) (n = 33 and 13 for NMI and MI disease, respectively; n = 62 and 9 for NMI and MI disease, respectively). Processed data were downloaded from NCBI GEO and/or an online publication supplement (44, 45). For visualization, cases from the Dyrskjot (47) cohort were clustered by expression of GDI2-regulated probes differentially expressed between NMI and MI cases in MATLAB, using Euclidean distance and average linkage. Correlation coefficient (rho) for rank-based Spearman's correlation of expression of indicated genes was used where indicated.

For plotting, $\log_2$ data for individual probes were standardized (z scored) before plotting values for NMI and MI tumors in Prism 5.0 (GraphPad Software), testing differences in distributions by the Mann-Whitney U test. On the Affymetrix HG-U133 platform, where multiple probes exist for *Vcan*, $\log_2$ data for probes were standardized (z scored), then averaged. For Kaplan-Meier analysis of the relationship between expression of *Vcan* and DSS, log-rank tests of differences in DSS by gene expression class (high or low expressor) were performed in MATLAB. The DSS curves presented use cutoffs at the optimal discriminating point for stratification of survival, with log-rank P values shown. The relative strength of association of GDI2 or *Vcan* expression to survival was further tested in multivariate Cox proportional hazard regression models, also in MATLAB.

IHC. Association of versican expression with tumor stage was evaluated using Wilcoxon-Mann-Whitney and Kruskal-Wallis tests (87, 88). Associations with DSS (DSS) were evaluated using the log-rank test. DSS time was defined as the months elapsed between transurethral resection or cystectomy and death of disease. Survival curves were plotted using Kaplan-Meier methodology, and statistical analyses were performed using the SPSS statistical package (IBM), version 18.0 (48, 87, 88).

Unless otherwise stated, all other data were statistically analyzed by 2-tailed Student's t test, 1-way ANOVA, and χ^2 square tests using Microsoft Excel 7.0 and GraphPad Prism 5 for Windows (GraphPad Software). Differences were deemed significant at $P < 0.05$.

Study approval

All animal experiments were performed after approval of protocol and in compliance with guidelines of the Animal Care and Use Committee of the University of Virginia. Bladder cancer TMAs were constructed at the Spanish National Cancer Institute (87, 88). These arrays included primary urothelial cell carcinomas of the bladder belonging to patients recruited under Institutional Review Board–approved protocols; patients gave informed consent in studies referenced (87, 88).

Acknowledgments

This study was supported by NIH grant CA143971 to D. Theodorescu. The authors wish to thank Sharon Birdsall, John Sanders,

Jeremy Gatesman, Marya Dunlap-Brown, Debora Thomson, and Charles Owens for technical help with experiments.

Received for publication October 10, 2011, and accepted in revised form January 18, 2012.

Address correspondence to: Dan Theodorescu, Departments of Surgery and Pharmacology and Comprehensive Cancer Center, University of Colorado, 13001 E. 17th Place, MS F-434, Aurora, Colorado 80045, USA. Phone: 303.724.7135; Fax: 303.724.3162; E-mail: dan.theodorescu@ucdenver.edu.

1. Gildea JJ, et al. RhoGDI2 is an invasion and metastasis suppressor gene in human cancer. *Cancer Res*. 2002;62(22):6418–6423.
2. Theodorescu D, Sapinoso LM, Conaway MR, Oxford G, Hampton GM, Frierson HF Jr. Reduced expression of metastasis suppressor RhoGDI2 is associated with decreased survival for patients with bladder cancer. *Clin Cancer Res*. 2004;10(11):3800–3806.
3. Wu Y, Siadaty MS, Berens ME, Hampton GM, Theodorescu D. Overlapping gene expression profiles of cell migration and tumor invasion in human bladder cancer identify metallothionein 1E and nicotinamide N-methyltransferase as novel regulators of cell migration. *Oncogene*. 2008;27(52):6679–6689.
4. Dours-Zimmermann MT, Maurer K, Rauch U, Stoffel W, Fassler R, Zimmermann DR. Versican V2 assembles the extracellular matrix surrounding the nodes of ranvier in the CNS. *J Neurosci*. 2009; 29(24):7731–7742.
5. Dours-Zimmermann MT, Zimmermann DR. A novel glycosaminoglycan attachment domain identified in two alternative splice variants of human versican. *J Biol Chem*. 1994;269(52):32992–32998.
6. Dutt S, Cassoly E, Dours-Zimmermann MT, Matasci M, Stoeckli ET, Zimmermann DR. Versican V0 and V1 direct the growth of peripheral axons in the developing chick hindlimb. *J Neurosci*. 2011;31(14):5262–5270.
7. Dutt S, Kleber M, Matasci M, Sommer L, Zimmermann DR. Versican V0 and V1 guide migratory neural crest cells. *J Biol Chem*. 2006;281(17):12123–12131.
8. Zimmermann DR, Dours-Zimmermann MT. Extracellular matrix of the central nervous system: from neglect to challenge. *Histochem Cell Biol*. 2008; 130(4):635–653.
9. Asplund A, et al. Hypoxic regulation of secreted proteoglycans in macrophages. *Glycobiology*. 2010; 20(1):33–40.
10. Seidelmann SB, et al. Athsq1 is an atherosclerosis modifier locus with dramatic effects on lesion area and prominent accumulation of versican. *Arterioscler Thromb Vasc Biol*. 2008;28(12):2180–2186.
11. Wagsater D, et al. ADAMTS-4 and -8 are inflammatory regulated enzymes expressed in macrophage-rich areas of human atherosclerotic plaques. *Atherosclerosis*. 2008;196(2):514–522.
12. Wilson P, Drennon K, Tannock LR. Regulation of vascular proteoglycan synthesis by metabolic factors associated with diabetes. *J Investig Med*. 2007; 55(1):18–25.
13. Beck AH, Espinosa I, Gilks CB, van de Rijn M, West RB. The fibromatosis signature defines a robust stromal response in breast carcinoma. *Lab Invest*. 2008; 88(6):591–601.
14. Brown LF, et al. Vascular stroma formation in carcinoma in situ, invasive carcinoma, and metastatic carcinoma of the breast. *Clin Cancer Res*. 1999; 5(5):1041–1056.
15. Castronovo V, et al. Identification of specific reachable molecular targets in human breast cancer using a versatile ex vivo proteomic method. *Proteomics*. 2007;7(8):1188–1196.
16. Kischel P, et al. Versican overexpression in human breast cancer lesions: known and new isoforms for stromal tumor targeting. *Int J Cancer*. 2010; 126(3):640–650.
17. Koyama H, et al. Hyperproduction of hyaluronan in neu-induced mammary tumor accelerates angiogenesis through stromal cell recruitment: possible involvement of versican/PG-M. *Am J Pathol*. 2007; 170(3):1086–1099.
18. Makatsori E, et al. Large matrix proteoglycans, versican and perlecan, are expressed and secreted by human leukemic monocytes. *Anticancer Res*. 2003;23(4):3303–3309.
19. Read JT, Rahmani M, Boroomand S, Allahverdian S, McManus BM, Rennie PS. Androgen receptor regulation of the versican gene through an androgen response element in the proximal promoter. *J Biol Chem*. 2007;282(44):31954–31963.
20. Ricciardelli C, et al. Regulation of stromal versican expression by breast cancer cells and importance to relapse-free survival in patients with node-negative primary breast cancer. *Clin Cancer Res*. 2002; 8(4):1054–1060.
21. Serra M, et al. V3 versican isoform expression alters the phenotype of melanoma cells and their tumorigenic potential. *Int J Cancer*. 2005;114(6):879–886.
22. Suwiwat S, et al. Expression of extracellular matrix components versican, chondroitin sulfate, tenascin, and hyaluronan, and their association with disease outcome in node-negative breast cancer. *Clin Cancer Res*. 2004;10(7):2491–2498.
23. Yee AJ, et al. The effect of versican G3 domain on local breast cancer invasiveness and bony metastasis. *Breast Cancer Res*. 2007;9(4):R47.
24. Yoon H, et al. Gene expression profiling of isogenic cells with different TP53 gene dosage reveals numerous genes that are affected by TP53 dosage and identifies CSPG2 as a direct target of p53. *Proc Natl Acad Sci U S A*. 2002;99(24):15632–15637.
25. Wu Y, McRoberts K, Berr SS, Frierson HF Jr, Conaway M, Theodorescu D. Neuromedin U is regulated by the metastasis suppressor RhoGDI2 and is a novel promoter of tumor formation, lung metastasis and cancer cachexia. *Oncogene*. 2007;26(5):765–773.
26. Chiodoni C, Colombo MP, Sangaletti S. Matricellular proteins: from homeostasis to inflammation, cancer, and metastasis. *Cancer Metastasis Rev*. 2010;29(2):295–307.
27. Rahmani M, et al. Versican: signaling to transcriptional control pathways. *Can J Physiol Pharmacol*. 2006;84(1):77–92.
28. Allavena P, Sica A, Solinas G, Porta C, Mantovani A. The inflammatory micro-environment in tumor progression: the role of tumor-associated macrophages. *Crit Rev Oncol Hematol*. 2008;66(1):1–9.
29. Wight TN. Versican: a versatile extracellular matrix proteoglycan in cell biology. *Curr Opin Cell Biol*. 2002;14(5):617–623.
30. Bhardwaj A, Frankel WL, Pellegata NS, Wen P, Prasad ML. Intracellular versican expression in mesenchymal spindle cell tumors contrasts with extracellular expression in epithelial and other tumors--a tissue microarray-based study. *Appl Immunohistochem Mol Morphol*. 2008;16(3):263–266.
31. Bouterfa H, Darlapp AR, Klein E, Pietsch T, Roosen K, Tonn JC. Expression of different extracellular matrix components in human brain tumor and melanoma cells in respect to variant culture conditions. *J Neurooncol*. 1999;44(1):23–33.
32. de Kluijver J, et al. Bronchial matrix and inflammation respond to inhaled steroids despite ongoing allergen exposure in asthma. *Clin Exp Allergy*. 2005;35(10):1361–1369.
33. Delpech B, et al. The origin of hyaluronectin in human tumors. *Int J Cancer*. 1997;72(6):942–948.
34. Docampo MJ, Rabanal RM, Miquel-Serra L, Hernandez D, Domenzain C, Bassols A. Altered expression of versican and hyaluronan in melanocytic tumors of dogs. *Am J Vet Res*. 2007;68(12):1376–1385.
35. Domenzain C, Docampo MJ, Serra M, Miquel L, Bassols A. Differential expression of versican isoforms is a component of the human melanoma cell differentiation process. *Biochim Biophys Acta*. 2003; 1642(1–2):107–114.
36. Domenzain-Reyna C, et al. Structure and regulation of the versican promoter: the versican promoter is regulated by AP-1 and TCF transcription factors in invasive human melanoma cells. *J Biol Chem*. 2009;284(18):12306–12317.
37. Touab M, Villena J, Barranco C, Arumi-Uria M, Bassols A. Versican is differentially expressed in human melanoma and may play a role in tumor development. *Am J Pathol*. 2002;160(2):549–557.
38. Rahmani M, et al. Regulation of the versican promoter by the beta-catenin-T-cell factor complex in vascular smooth muscle cells. *J Biol Chem*. 2005; 280(13):13019–13028.
39. Serra M, Pastor J, Domenzain C, Bassols A. Effect of transforming growth factor-beta1, insulin-like growth factor-I, and hepatocyte growth factor on proteoglycan production and regulation in canine melanoma cell lines. *Am J Vet Res*. 2002;63(8):1151–1158.
40. Smith SC, Theodorescu D. Learning therapeutic lessons from metastasis suppressor proteins. *Nat Rev Cancer*. 2009;9(4):253–264.
41. Steeg PS, Horak CE, Miller KD. Clinical-translational approaches to the Nm23-H1 metastasis suppressor. *Clin Cancer Res*. 2008;14(16):5006–5012.
42. Moissoglu K, McRoberts KS, Meier JA, Theodorescu D, Schwartz MA. Rho GDP dissociation inhibitor 2 suppresses metastasis via unconventional regulation of RhoGTPases. *Cancer Res*. 2009; 69(7):2838–2844.
43. Dyrskjot L, et al. Gene expression in the urinary bladder: a common carcinoma in situ gene expression signature exists disregarding histopathological classification. *Cancer Res*. 2004;64(11):4040–4048.
44. Sanchez-Carbayo M, Socci ND, Lozano J, Saint F, Cordon-Cardo C. Defining molecular profiles of poor outcome in patients with invasive bladder cancer using oligonucleotide microarrays. *J Clin Oncol*. 2006; 24(5):778–789.
45. Stransky N, et al. Regional copy number-independent deregulation of transcription in cancer. *Nat Genet*. 2006;38(12):1386–1396.
46. Kim WJ, et al. Predictive value of progression-related gene classifier in primary non-muscle invasive bladder cancer. *Mol Cancer*. 2010;9:3.
47. Dyrskjot L, et al. Identifying distinct classes of bladder carcinoma using microarrays. *Nat Genet*. 2003;33(1):90–96.
48. Said N, Smith S, Sanchez-Carbayo M, Theodorescu D. Tumor endothelin-1 enhances metastatic colonization of the lung in mouse xenograft models of bladder cancer. *J Clin Invest*. 2011;121(1):132–147.
49. Qian BZ, et al. CCL2 recruits inflammatory monocytes to facilitate breast-tumour metastasis. *Nature*. 2011;475(7355):222–225.
50. Kim S, et al. Carcinoma-produced factors activate myeloid cells through TLR2 to stimulate metastasis. *Nature*. 2009;457(7225):102–106.
51. Farb A, et al. Extracellular matrix changes in stented human coronary arteries. *Circulation*. 2004; 110(8):940–947.
52. Lemire JM, Merrilees MJ, Braun KR, Wight TN. Overexpression of the V3 variant of versican alters arterial smooth muscle cell adhesion, migration, and proliferation in vitro. *J Cell Physiol*. 2002;190(1):38–45.
53. Osada S, Hamada C, Shimaoka T, Kaneko K, Horikoshi S, Tomino Y. Alterations in proteoglycan components and histopathology of the peritoneum

in uraemic and peritoneal dialysis (PD) patients. *Nephrol Dial Transplant*. 2009;24(11):3504–3512.
54. Potter-Perigo S, et al. Poly I:C stimulates versican accumulation in the extracellular matrix promoting monocyte adhesion. *Am J Respir Cell Mol Biol*. 2010;43(1):109–120.
55. Hagemann T, Robinson SC, Schulz M, Trumper L, Balkwill FR, Binder C. Enhanced invasiveness of breast cancer cell lines upon co-cultivation with macrophages is due to TNF-alpha dependent up-regulation of matrix metalloproteases. *Carcinogenesis*. 2004;25(8):1543–1549.
56. Said N, Socha MJ, Olearczyk JJ, Elmarakby AA, Imig JD, Motamed K. Normalization of the ovarian cancer microenvironment by SPARC. *Mol Cancer Res*. 2007;5(10):1015–1030.
57. Condeelis J, Pollard JW. Macrophages: obligate partners for tumor cell migration, invasion, and metastasis. *Cell*. 2006;124(2):263–266.
58. Pollard JW. Tumour-educated macrophages promote tumour progression and metastasis. *Nat Rev Cancer*. 2004;4(1):71–78.
59. Hagemann T, et al. Macrophages induce invasiveness of epithelial cancer cells via NF-kappa B and JNK. *J Immunol*. 2005;175(2):1197–1205.
60. Mantovani A, Sica A, Allavena P, Garlanda C, Locati M. Tumor-associated macrophages and the related myeloid-derived suppressor cells as a paradigm of the diversity of macrophage activation. *Hum Immunol*. 2009;70(5):325–330.
61. Kulbe H, Hagemann T, Szlosarek PW, Balkwill FR, Wilson JL. The inflammatory cytokine tumor necrosis factor-alpha regulates chemokine receptor expression on ovarian cancer cells. *Cancer Res*. 2005;65(22):10355–10362.
62. Roca H, Varsos ZS, Sud S, Craig MJ, Ying C, Pienta KJ. CCL2 and interleukin-6 promote survival of human CD11b+ peripheral blood mononuclear cells and induce M2-type macrophage polarization. *J Biol Chem*. 2009;284(49):34342–34354.
63. Zhang J, Patel L, Pienta KJ. CC chemokine ligand 2 (CCL2) promotes prostate cancer tumorigenesis and metastasis. *Cytokine Growth Factor Rev*. 2010; 21(1):41–48.
64. Goueffic Y, et al. Sirolimus blocks the accumulation of hyaluronan (HA) by arterial smooth muscle cells and reduces monocyte adhesion to the ECM. *Atherosclerosis*. 2007;195(1):23–30.
65. Lu X, Kang Y. Chemokine (C-C motif) ligand 2 engages CCR2+ stromal cells of monocytic origin to promote breast cancer metastasis to lung and bone. *J Biol Chem*. 2009;284(42):29087–29096.
66. Piccinini AM, Knebl K, Rek A, Wildner G, Diedrichs-Mohring M, Kungl AJ. Rationally evolving MCP-1/CCL2 into a decoy protein with potent anti-inflammatory activity in vivo. *J Biol Chem*. 2010; 285(12):8782–8792.
67. Wisniewski T, et al. Assessment of chemokine receptor function on monocytes in whole blood: In vitro and ex vivo evaluations of a CCR2 antagonist. *J Immunol Methods*. 2010;352(1–2):101–110.
68. Said N, Theodorescu D. Pathways of metastasis suppression in bladder cancer. *Cancer Metastasis Rev*. 2009;28(3–4):327–333.
69. Witz IP. Tumor-microenvironment interactions: dangerous liaisons. *Adv Cancer Res*. 2008;100:203–229.
70. Mantovani A. Cancer: Inflaming metastasis. *Nature*. 2009;457(7225):36–37.
71. Miquel-Serra L, et al. V3 versican isoform expression has a dual role in human melanoma tumor growth and metastasis. *Lab Invest*. 2006;86(9):889–901.
72. Loberg RD, et al. CCL2 is a potent regulator of prostate cancer cell migration and proliferation. *Neoplasia*. 2006;8(7):578–586.
73. Loberg RD, et al. Targeting CCL2 with systemic delivery of neutralizing antibodies induces prostate cancer tumor regression in vivo. *Cancer Res*. 2007; 67(19):9417–9424.
74. Rozel S, et al. Synergy between anti-CCL2 and docetaxel as determined by DW-MRI in a metastatic bone cancer model. *J Cell Biochem*. 2009;107(1):58–64.
75. Said NA, Elmarakby AA, Imig JD, Fulton DJ, Motamed K. SPARC ameliorates ovarian cancer-associated inflammation. *Neoplasia*. 2008;10(10):1092–1104.
76. Zhang J, Lu Y, Pienta KJ. Multiple roles of chemokine (C-C motif) ligand 2 in promoting prostate cancer growth. *J Natl Cancer Inst*. 2010;102(8):522–528.
77. Thompson WL, Van Eldik LJ. Inflammatory cytokines stimulate the chemokines CCL2/MCP-1 and CCL7/MCP-3 through NFkB and MAPK dependent pathways in rat astrocytes [corrected]. *Brain Res*. 2009;1287:47–57.
78. Said NA, Najwer I, Socha MJ, Fulton DJ, Mok SC, Motamed K. SPARC inhibits LPA-mediated mesothelial-ovarian cancer cell crosstalk. *Neoplasia*. 2007;9(1):23–35.
79. Thacker MA, et al. CCL2 is a key mediator of microglia activation in neuropathic pain states. *Eur J Pain*. 2009;13(3):263–272.
80. Wu Y, et al. Src phosphorylation of RhoGDI2 regulates its metastasis suppressor function. *Proc Natl Acad Sci U S A*. 2009;106(14):5807–5812.
81. Moon HG, et al. Up-regulation of RhoGDI2 in human breast cancer and its prognostic implications. *Cancer Res Treat*. 2010;42(3):151–156.
82. Li X, Wang J, Zhang X, Zeng Y, Liang L, Ding Y. Overexpression of RhoGDI2 correlates with tumor progression and poor prognosis in colorectal carcinoma. *Ann Surg Oncol*. 2012;19(1):145–153.
83. Naso MF, Zimmermann DR, Iozzo RV. Characterization of the complete genomic structure of the human versican gene and functional analysis of its promoter. *J Biol Chem*. 1994;269(52):32999–33008.
84. Sheng W, Dong H, Lee DY, Lu WY, Yang BB. Versican modulates gap junction intercellular communication. *J Cell Physiol*. 2007;211(1):213–219.
85. Sheng W, et al. The roles of versican V1 and V2 isoforms in cell proliferation and apoptosis. *Mol Biol Cell*. 2005;16(3):1330–1340.
86. Mukhopadhyay A, et al. Erosive vitreoretinopathy and wagner disease are caused by intronic mutations in CSPG2/Versican that result in an imbalance of splice variants. *Invest Ophthalmol Vis Sci*. 2006; 47(8):3565–3572.
87. Orenes-Pinero E, et al. Serum and tissue profiling in bladder cancer combining protein and tissue arrays. *J Proteome Res*. 2010;9(1):164–173.
88. Ruppen I, et al. Differential protein expression profiling by iTRAQ-two-dimensional LC-MS/MS of human bladder cancer EJ138 cells transfected with the metastasis suppressor KiSS-1 gene. *Mol Cell Proteomics*. 2010;9(10):2276–2291.